GEOPHYSICAL RESEARCH LETTERS, VOL. 37, L06706, doi:10.1029/2009GL042225, 2010

Mid-Brunhes strengthening of the Indian Ocean Dipole caused increased equatorial East African and decreased Australasian rainfall

Anil K. Gupta,[1] Sudipta Sarkar,[1] Soma De,[1] Steven C. Clemens,[2] and Angamuthu Velu[1]

Received 18 December 2009; accepted 18 February 2010; published 23 March 2010.

[1] The tropical Indian Ocean is an important component of the largest warm pool, marked by changes in sea surface temperatures and depths of thermocline and mixed layer in its western and eastern extremities leading to the development of a dipole mode - the Indian Ocean Dipole (IOD). A narrow band of westerlies (7°N to 7°S) sweep the equatorial Indian Ocean during the April–May and October–November transitions between the summer- and winter-monsoon seasons. These Indian Ocean equatorial westerlies (IEW) are closely related to the IOD, intensifying the upper ocean Eastward Equatorial current also known as Wyrtki jets. The strength of the IOD/IEW determines the moisture content in East Africa. A major decrease in the strength of the IEW (strengthening or positive mode of the IOD) during the mid-Brunhes epoch (~300–250 Kyr BP) coincides with a wetter equatorial East Africa, a drier Australasia and a stronger Indian summer monsoon, indicating that the IOD/IEW play a significant role in driving climate change in East Africa, Australasia and South Asia. **Citation:** Gupta, A. K., S. Sarkar, S. De, S. C. Clemens, and A. Velu (2010), Mid-Brunhes strengthening of the Indian Ocean Dipole caused increased equatorial East African and decreased Australasian rainfall, *Geophys. Res. Lett.*, *37*, L06706, doi:10.1029/2009GL042225.

1. Introduction

[2] The tropics play a crucial role in modulating regional and global climates owing to their large heat and moisture storage capacity [*Hastenrath et al.*, 1993; *Schott et al.*, 2009]. The tropical Indian Ocean forms the major part of the largest warm pool on Earth, and its interaction with the atmosphere triggers important climate variations on both regional and global scales [*Schott et al.*, 2009]. The atmospheric and oceanic circulation in the Indian Ocean is dominated by the complete reversal of wind field between summer and winter. This has led to most meteorological and oceanographic research traditionally focusing on the two monsoon periods especially the boreal summer monsoon, with strongest winds, abundant rainfall and latent heat released over southern Asia. In contrast, the equatorial Indian Ocean is marked by weak winds during monsoon seasons and stronger winds during monsoon transitions in April–May and October–November [*Clark et al.*, 2003; *Hastenrath and Greischar*, 1992]. Most of equatorial East Africa experiences rainy seasons during the boreal spring (April–May) and autumn (October–November) monsoon transitions. The spring rainfall is usually more abundant and of longer duration whereas that of autumn is less abundant and more variable [*Clark et al.*, 2003; *Hastenrath and Greischar*, 1992]. Strong westerly winds called the Indian Ocean equatorial westerlies (IEW) sweep the equatorial zone of the Indian Ocean during April–May and October–November (Figure 1) which drive the Eastward Equatorial current (EEC) known as Wyrtki jets in the upper ocean [*Hastenrath et al.*, 1993; *Wyrtki*, 1973]. The IEW and EEC are stronger and more variable in October–November (deficient rains) than in April–May (abundant rains). With stronger westerlies, the EEC is accelerated transporting warmer upper layer water towards the east thickening the mixed layer and thermocline through convergence in the eastern equatorial Indian Ocean but reducing them in the western equatorial Indian Ocean through divergent upwelling. Enhanced convergence in the east is associated with warm sea surface temperatures (SST) while enhanced divergence in the west is associated with cold SST.

[3] The strength of the coupled IEW/EEC system is closely related to positive and negative modes of the Indian Ocean Dipole (IOD) – a phenomenon that occurs interannually due to basin-wide ocean-atmosphere coupled dynamics [*Saji et al.*, 1999; *Webster et al.*, 1999] and impacts climate conditions in many parts of the world [*Saji and Yamagata*, 2003]. The positive mode of the IOD is marked by unusually warmer SSTs (deep thermocline) over large parts of the western Indian Ocean and cooler SSTs (shallow thermocline) in the southeastern Indian Ocean off Sumatra [*Saji et al.*, 1999]. This weakens the IEW and reverses the direction of the equatorial surface winds (to easterlies), causing heavy rains and floods over equatorial East Africa and deficient rainfall over Australasia [*Saji et al.*, 1999]. At the seasonal time scale, monsoon reversals are responsible for the disappearance of positive dipole mode events and appearance of the negative dipole modes as stronger summer monsoon winds induce greater mixing and greater Ekman transport forcing strong coastal upwelling, all of which contribute to rapid cooling in the west [*Saji et al.*, 1999].

[4] Although the IEW (monsoon transitions) and the IOD are of significant climatic importance, no fruitful attempt has yet been made to understand their impact on climate of the African and Australasian regions in the past, particularly during the late Quaternary. The only high resolution study

[1]Department of Geology and Geophysics, Indian Institute of Technology, Kharagpur, India.
[2]Department of Geological Sciences, Brown University, Providence, Rhode Island, USA.

0094-8276/10/2009GL042225

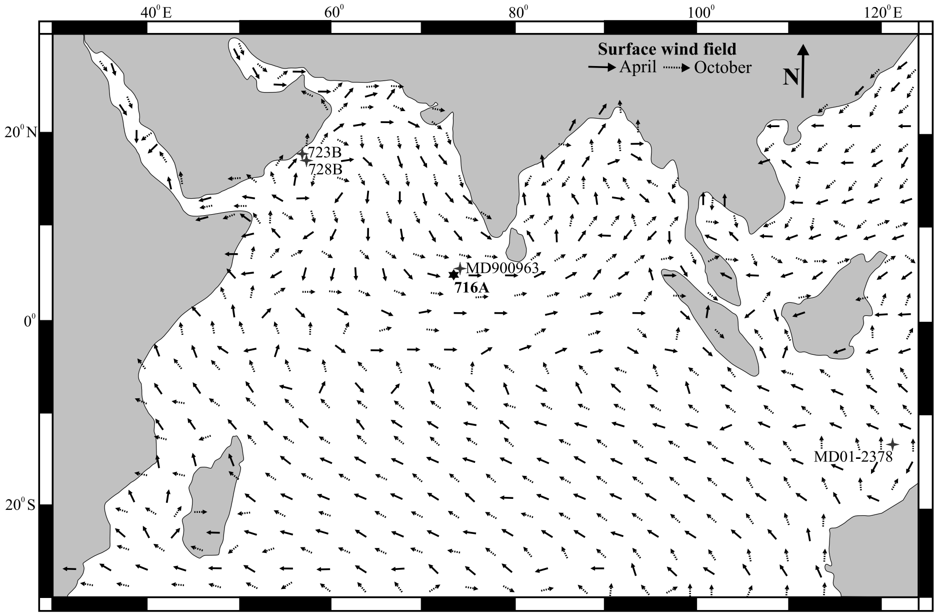

Figure 1. Location of ODP Holes 716A, 723B, 728B and core MD900963 with wind fields during April and October [*Hastenrath and Greischar*, 1992]. Hole 716A lies on the Maldives Ridge below a narrow band of the intense Indian Ocean equatorial westerlies (IEW).

from the late Quaternary of the equatorial Indian Ocean is from core MD900963, located near Chagos-Laccadive Ridge [*Beaufort et al.*, 1997]. This study identifies a relation between solar insolation and IEW intensity driving productivity changes in the equatorial Indian Ocean independent of global ice volume changes. *Beaufort et al.* [1997] suggested that changes in primary production in the equatorial Indian Ocean were driven by equatorial westerlies, which is related to precession forcing on Southern Oscillation (SO). Our study is directed toward understanding significance of the IOD/IEW in driving climate change in more distant regions surrounding the equatorial Indian Ocean. To understand if IOD/IEW variability has triggered climate change in the equatorial East Africa and Australasia or the Indonesian archipelago (including Indonesia, northern Australia, Malaysia and surrounding regions) during the late Quaternary, we generated proxy records including census data of planktic foraminifer *Globigerina bulloides* and benthic foraminifer *Cymbaloporetta squammosa* from 892 core samples as well as stable isotope values of *Globigerinoides ruber* from 200 samples from Ocean Drilling Program (ODP) Site 716, Hole A (Figure 2 and auxiliary material).[1] These proxies are combined with *G. bulloides* census data from Hole 728B (this study) and Hole 723B [*Emeis et al.*, 1995], stable isotope values from adjacent core MD900963 [*Beaufort et al.*, 1997] and vegetation records from the Timor Sea core MD01-2378 [*Kawamura et al.*, 2006] (Figure 2). The study of the IOD in paleo record has socio-economic relevance because equatorial East Africa and Indonesia as well as South Asia face possibility of climate surprises and abrupt changes in the precipitation budget of these regions will severely impact their agriculture-based economies.

2. Materials, Methods, and Results

[5] Site 716 is located on the broad central plateau of the Maldives Ridge, equatorial Indian Ocean (04°56.0′N; 73° 17.0′E; water depth 533.3 m) beneath the narrow track of the IEW (7°N to 7°S), providing a well-preserved late Quaternary record of climate variability in the tropical Indian Ocean (Figure 1). This site is ideally located to capture IOD/IEW-driven changes in the paleo record. Core samples were processed using standard procedures as described by *Gupta et al.* [2006]. The percent distribution of *Globigerina bulloides* was calculated out of ~300 specimens of planktic foraminifera from >149 μm size fraction whereas *Cymbaloporetta squammosa* was examined from benthic foraminiferal population from >125 μm size fraction of each sample following *Gupta et al.* [2006].

[6] Stable oxygen isotope ratios of *Globigerinoides ruber* sensu stricto (s.s.) at every 2 cm interval during 444–151 Kyr (kilo years) interval from Hole 716A were examined at Brown University, USA. About 40–50 specimens of *Gs. ruber* (s.s.) were picked from 212–355 μm size fraction from 200 samples for stable isotope analysis. Samples were run in batches of ~40 on a Finnigan MAT 252 equipped with a Carbonate (Kiel) III autosampler that reacts samples in individual reaction vessels at 70°C using H_3PO_4. Each sample consisted of 3 to 7 individuals of *Gs. ruber* from the 212–355 micron size fraction (precleaned by sonification in methanol). Samples were not run in stratigraphic order. Reproducibility based on repeated analysis internal laboratory standard (Carrara and Brown Yule marble, N = 24) is ±0.06‰ for δ^{18}O (1σ). The Carrara and Brown Yule standards have been calibrated to National Institute of Standards

[1] Auxiliary materials are available in the HTML. doi:10.1029/2009GL042225.

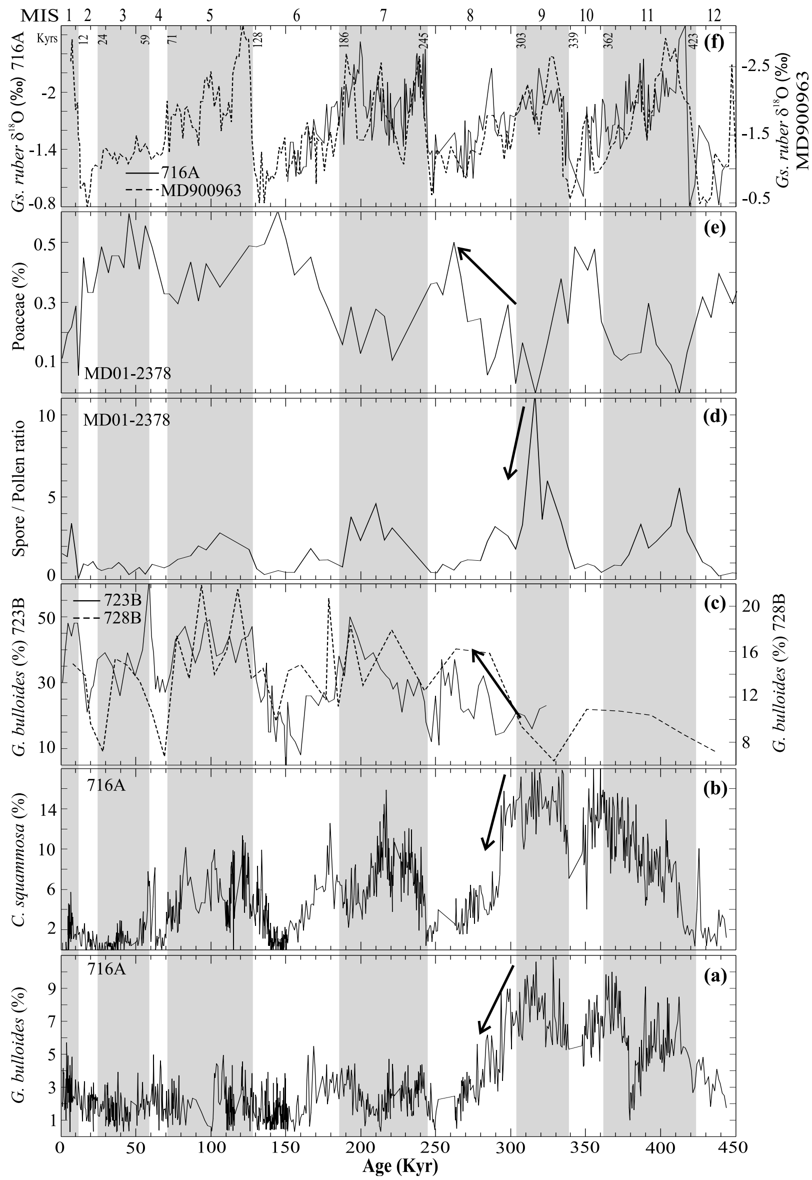

Figure 2. Proxy records from the equatorial Indian Ocean, NW Arabian Sea and Timor Sea. (a) Percent distribution of *Globigerina bulloides* at Hole 716A. A major decrease in *G. bulloides* percentages at ~300 Kyr coincides with a major shift in NW Arabian Sea, East African and Australasian climates; (b) benthic foraminifer *Cymbaloporetta squammosa* – an indicator of more productive waters, also shows a major decline at Hole 716A at ~300 Kyr; (c) *G. bulloides* percentages show a major increase at NW Arabian Sea Holes 723B [*Emeis et al.*, 1995] and 728B (this study) indicating intensification of the SW monsoon between ~300 and 250 Kyr. (d) A decrease in spore/pollen ratio and (e) an increase in *Poaceae* population at ~300–250 Kyr suggest the beginning of an arid phase in Australasia including Indonesia, northern Australia and adjacent regions [*Kawamura et al.*, 2006]; (f) oxygen isotope values of *Globigerinoides ruber* from Hole 716A and core MD900963 [*Beaufort et al.*, 1997] used to interpolate ages of the samples after tuning with the SPECMAP stacked record [*Imbrie et al.*, 1984]. Grey bars illustrate interglacial marine isotope stages (MIS).

and Technology (NIST) isotopic reference material NBS-19 for conversion to the (Vienna) Peedee Belemnite (VPDB) scale. All data reported here are relative to VPDB.

[7] The average time interval per studied sample is 498 years (ranging from 99–2000 years) based on linear interpolation of six AMS ^{14}C calibrated dates (up to 30.5 Kyr BP) and two nannofossil datums [*Backman et al.*, 1988]. The ages for the interval from 444 to 150 Kyrs are based on oxygen isotope values of *Globigerinoides ruber* from Hole 716A which show a close match with those from the adjacent core MD900963 (Figure 2f). The ages were estimated by tuning to the SPECMAP stacked $\delta^{18}O$ record of *Imbrie et al.* [1984] using AnalySeries 2.0.3 [*Paillard et al.*, 1996]. Holes 723B and 728B (Lat. 17°40.790′N; Long. 57°49.553′E; water depth 1428 m) are located in the NW Arabian Sea below an active upwelling cell.

[8] *Globigerina bulloides* is a near surface dwelling planktic foraminifer, conventionally known from the transitional and sub-polar water masses [*Bé*, 1977] but has also been found in significant proportions in tropical and subtropical wind-driven upwelling regions of the Indian Ocean [*Prell and Curry*, 1981]. This species produces high shell

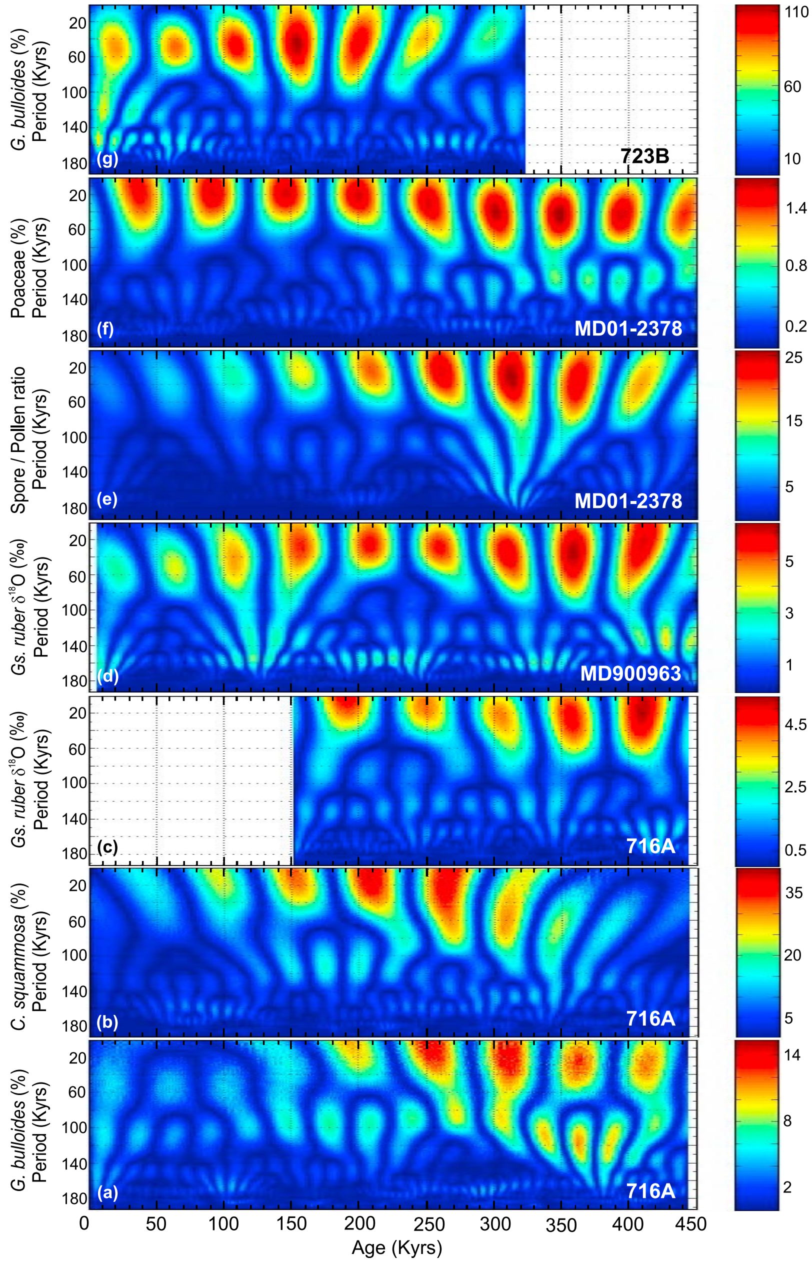

Figure 3. Continuous Wavelet Transform (CWT) was run on important climate proxy data from the equatorial Indian Ocean ODP Hole 716A, core MD900963 and Timor Sea core MD01-2378, applying Morlet wavelets using MATLAB 7.1 software. Prior to analysis, the values were interpolated at every 750 years age interval applying Piecewise cubic Hermite interpolation (pchip) on Matlab 7.1 platform. The data interpolation was consistent with the average temporal resolution of the respective data sets. (a) *Globigerina bulloides*, (b) *Cymbaloporetta squammosa* and δ^{18}O values of *Globigerinoides ruber* from (c) Hole 716A and (d) core MD900963 [*Beaufort et al.*, 1997], (e) spores and pollen ratio and (f) *Poaceae* population from core MD01-2378 [*Kawamura et al.*, 2006], and (g) *Globigerina bulloides* from Hole 723A [*Emeis et al.*, 1995] show a change from low-frequency to high-frequency (precessional peak) across the mid-Brunhes Climatic Event (300–250 Kyr BP).

fluxes in high-productivity monsoon regimes of the tropical NW Indian Ocean including the Arabian Sea and has widely been used in determining southwest monsoon wind intensities during the late Quaternary and the Holocene [*Anderson and Prell*, 1993; *Gupta et al.*, 2003]. Benthic foraminifer *Cymbaloporetta squammosa*, a characteristic upper bathyal species, follows *G. bulloides* population trend indicating that this species prefers habitat beneath more productive surface waters (Figure 2b). The late Quaternary record of *G. bulloides* and *C. squammosa* at Hole 716A shows a major decrease in their population at ~300–250 Kyr BP coinciding with vegetation changes in the equatorial East Africa and Australasia (Figure 2).

3. Discussion and Conclusions

[9] We interpret the abrupt decrease in *G. bulloides* population during the middle Brunhes epoch across MIS 9

and 8 (~300–250 Kyr) at Hole 716A as a major decrease in IEW strength and increase (positive mode) in IOD strength with consequent climate change in the surrounding equatorial regions including East Africa and Australasia (Figure 2). The IEW remained weak following the mid-Brunhes transition with significantly reduced variability, suggesting an overall strengthened (positive) IOD. Our interpretation is supported by vegetation changes in the regions east and west of the Indian Ocean. Prior to the transition, Australasia experienced wet conditions (~460 to ~300 Kyr BP) (Figures 2d and 2e) [*Kawamura et al.*, 2006] whereas tropical Africa experienced dry conditions [*Jansen et al.*, 1986] consistent with a strengthened IEW and negative IOD condition. The inferred mid-Brunhes (300–250 Kyr) weakening of the IEW (strengthening of the IOD) coincides with a shift towards dry conditions in Australasia marked by the replacement of araucarian forest by eucalypt woodland leading to frequent forest fires [*Kershaw et al.*, 2005]. A study from Timor Sea also indicates increase in grassland taxa after 300 Kyr, which grow in low precipitation conditions [*Kawamura et al.*, 2006]. This event has been linked to an abrupt drop in precipitation levels in Australia around 300 Kyr BP [*Kershaw et al.*, 2003], during which time equatorial East Africa turned wetter [*Jansen et al.*, 1986] and the Indian summer monsoon intensified (increased *G. bulloides* population at holes 723B [*Emeis et al.*, 1995] and 728B, NW Arabian Sea (Figure 2c). Recent observations on the Indian Ocean SST found a stronger link of East African rainfall with the IOD than with the tropical Pacific [*Saji et al.*, 1999; *Black*, 2005]. In a recent study, *Abram et al.* [2007] observed a positive relation between ENSO-independent strengthening of the Asian monsoon and IOD-related droughts in the Australian-Indonesian region during the early to middle Holocene. The positive mode of the IOD supports the transport of moisture by easterlies towards India enhancing amount of rainfall in the region [*Kripalani and Kumar*, 2004].

[10] The mid-Brunhes climate event has widely been reported from the Pacific [*Schramm*, 1985; *Pisias and Rea*, 1988; *Rea*, 1990]. This event was originally observed by *Jansen et al.* [1986], marked by warm conditions in the southern hemisphere and cold periods in the northern hemisphere. In the eastern Pacific, this event was followed by lower variability in SST and other climate proxies [*Pisias and Rea*, 1988], which is similar to the record from Hole 716A. The exact cause of this event remains uncertain: an asymmetrical response to eccentricity [*Jansen et al.*, 1986] and a change in the West Pacific Warm Pool (WPWP) surface temperatures linked with El Niño-Southern Oscillation or ENSO [*Isern et al.*, 1996] have been suggested as potential drivers. *Behera and Yamagata* [2003], however, showed that the SO is also influenced by the IOD through its influence on the pressure at Darwin.

[11] We propose a hypothesis linking weakening of the IEW or a switch towards positive mode of the IOD during 300–250 Kyr to a weak SO phase which may have caused abundant rainfall in equatorial East Africa and droughts in Australasia. *Hastenrath et al.* [1993] suggested that the high-SO phase is associated with low pressure over the Indian Ocean, anomalously warm waters in the Indonesian region, and a cold western Indian Ocean (negative IOD), accelerating the IEW. During the weak (negative-) -SO phase, the tropical Pacific is characterized by weaker easterlies, and Indonesian waters are colder. The proxy response at Hole 716A and cores MD900963 and MD01-2378 changed from low frequency to high frequency cycles with a shift towards stronger precessional signal across the mid-Brunhes epoch (Figure 3). It is therefore likely that a weak SO phase was related to a change in solar insolation. A change in the primary production in the equatorial Indian Ocean was linked to precessional forcing on the SO [*Beaufort et al.*, 1997]. The higher SSTs in the west increased the tropical evaporation and the atmospheric moisture content at ~300–250 Kyr which was the main source of the African precipitation. We further suggest that changes in the depth of the thermocline or thickness of the mixed layer in the east and west equatorial Indian Ocean resulted from variability in the IOD/IEW strength.

[12] We report evidence of the mid-Brunhes climatic event for the first time from the equatorial Indian Ocean, and establish a link between long-term IOD dynamics and climate of the Indian Ocean region in the paleo record. The coincidence of increased equatorial East African precipitation and drying of Australasia across the middle Brunhes corroborate our interpretation and indicate that the IOD/IEW have been major forcing factors driving significant climatic changes in the Indian Ocean region during the late Quaternary. These interpretations are consistent with the recent model results and observational records [*Saji et al.*, 1999; *Webster et al.*, 1999] linking IOD with the rainfall in the East African and Australasian (Indonesian) regions.

[13] **Acknowledgments.** AKG thanks Integrated Ocean Drilling Program for providing samples (under IODP request 17649E) for the present study. This study was supported by the Department of Science and Technology, New Delhi to AKG (SR/S4/ES-46/2003 and SR/S4/ES-304/2007) and Council of Scientific and Industrial Research (CSIR), New Delhi through independent scholarships to SS and SD. The authors thank two anonymous reviewers for constructive comments on an earlier version of the manuscript.

References

Abram, N. J., M. K. Gagan, Z. Liu, W. S. Hantoro, M. T. McCulloch, and B. W. Suwargadi (2007), Seasonal characteristics of the Indian Ocean Dipole during the Holocene epoch, *Nature*, *445*, 299–302, doi:10.1038/nature05477.

Anderson, D. M., and W. L. Prell (1993), A 300 kyr record of upwelling off Oman during the Late Quaternary: evidence of the Asian southwest monsoon, *Paleoceanography*, *8*(2), 193–208, doi:10.1029/93PA00256.

Backman, J., et al. (1988), Chapter 13, Site 716, *Proc. Ocean Drilling Prog.*, *115*, 1005–1073.

Bé, A. W. H. (1977), An ecological, zoogeographic and taxonomic review of recent planktonic foraminifera, in *Oceanic Micropaleontology*, vol. 1, edited by A. T. S. Ramsay, pp. 1–100, Academic, London.

Beaufort, L., Y. Lancelot, P. Camberlin, O. Cayre, E. Vincent, F. Bassinot, and L. Labeyrie (1997), Insolation cycles as a major control of equatorial Indian Ocean primary production, *Science*, *278*, 1451–1454, doi:10.1126/science.278.5342.1451.

Behera, S. K., and T. Yamagata (2003), Influence of the Indian Ocean Dipole on the Southern Oscillation, *J. Meteorol. Soc. Jpn.*, *81*, 169–177, doi:10.2151/jmsj.81.169.

Black, E. (2005), The relationship between Indian Ocean sea-surface temperature and east African rainfall, *Philos. Trans. R. Soc., Ser. A*, *363*, 43–47, doi:10.1098/rsta.2004.1474.

Clark, C. O., P. J. Webster, and J. E. Cole (2003), Interdecadal variability of the relationship between the Indian Ocean zonal mode and East African coastal rainfall anomalies, *J. Clim.*, *16*, 548–554, doi:10.1175/1520-0442(2003)016<0548:IVOTRB>2.0.CO;2.

Emeis, K.-C., D. M. Anderson, H. Doose, D. Kroon, and D. Schulz-Bull (1995), Sea-surface temperatures and the history of monsoon upwelling in the northwest Arabian Sea during the last 500,000 years, *Quat. Res.*, *43*, 355–361, doi:10.1006/qres.1995.1041.

Gupta, A. K., D. M. Anderson, and J. T. Overpeck (2003), Abrupt changes in the Asian southwest monsoon during the Holocene and their links to the North Atlantic Ocean, *Nature*, *421*, 354–357, doi:10.1038/nature01340.

Gupta, A. K., S. Sarkar, and B. Mukherjee (2006), Deep-sea paleoceanographic changes at DSDP Site 238, Central Indian Ocean Basin during the past 1.9 Myr: Benthic foraminiferal proxies, *Mar. Micropaleontol.*, *60*, 157–166, doi:10.1016/j.marmicro.2006.04.001.

Hastenrath, S., and L. Greischar (1992), Studies on the upper-hydrospheric climate of the tropical Indian Ocean, *Trends Phys. Oceanogr.*, *1*, 181–208.

Hastenrath, S., A. Nicklis, and L. Greischar (1993), Atmospheric-Hydrospheric mechanisms of climate anomalies in the western equatorial Indian Ocean, *J. Geophys. Res.*, *98*, 20,219–20,235, doi:10.1029/93JC02330.

Imbrie, J., D. Hays, D. G. Martinson, A. McIntyre, A. C. Mix, J. J. Morley, N. G. Pisias, W. L. Prell, and N. J. Shackleton (1984), The orbital theory of Pleistocene climate: support from a revised chronology of the marine δ^{18}O record, in *Milankovitch and Climate*, *NATO ASI Ser. C*, vol. 1, edited by A. Berger et al., Reidel, pp. 269–306, Dordrecht, Netherlands.

Isern, A. R., J. A. McKenzie, and D. A. Feary (1996), The role of sea surface temperature as a control on carbonate platform development in the western Coral Sea, *Palaeogeogr. Palaeoclimatol. Palaeoecol.*, *124*, 247–272, doi:10.1016/0031-0182(96)80502-5.

Jansen, J. H. F., A. Kuijpers, and S. R. Troelstra (1986), A Mid-Brunhes climatic event: long-term changes in global atmosphere and ocean circulation, *Science*, *232*, 619–622, doi:10.1126/science.232.4750.619.

Kawamura, H., A. Holbourn, and W. Kuhnt (2006), Climate variability and land-ocean interactions in the Indo Pacific Warm Pool: A 460-ka palynological and organic geochemical record from the Timor Sea, *Mar. Micropaleontol.*, *59*, 1–14, doi:10.1016/j.marmicro.2005.09.001.

Kershaw, A. P., S. van der Kaars, and P. T. Moss (2003), Late Quaternary Milankovitch-scale climatic change and variability and its impact on monsoonal Australasia, *Mar. Geol.*, *201*, 81–95, doi:10.1016/S0025-3227(03)00210-X.

Kershaw, A. P., P. T. Moss, and R. Wild (2005), Patterns and causes of vegetation change in the Australian wet tropics region over the last 10 million years, in *Tropical Rainforests: Past and Future*, edited by E. Bermingham, C. W. Dick, and C. Moritz, pp. 375–400, Univ. Chicago Press, Chicago, Ill.

Kripalani, R. H., and P. Kumar (2004), Northeast rainfall variability over South Peninsular India vis-à-vis the Indian Ocean Dipole mode, *Int. J. Climatol.*, *24*, 1267–1282, doi:10.1002/joc.1071.

Paillard, D., L. Labeyrie, and P. Yiou (1996), Macintosh program performs time-series analysis, *Eos Trans. AGU*, *77*, 379, doi:10.1029/96EO00259.

Pisias, N. G., and D. K. Rea (1988), Late Pleistocene paleoclimatology of the central equatorial Pacific: sea surface response to the southeast trade winds, *Paleoceanography*, *3*, 21–37, doi:10.1029/PA003i001p00021.

Prell, W. L., and W. B. Curry (1981), Faunal and isotopic indices of monsoonal upwelling: western Arabian Sea, *Oceanol. Acta*, *4*, 91–98.

Rea, D. K. (1990), Aspects of atmospheric circulation: the Late Pleistocene (0–950,000 Yr) record of eolian deposition in the Pacific Ocean, *Palaeogeogr. Palaeoclimatol. Palaeoecol.*, *78*, 217–227, doi:10.1016/0031-0182(90)90215-S.

Saji, N. H., and T. Yamagata (2003), Possible impacts of Indian Ocean Dipole mode events on global climate, *Clim. Res.*, *25*, 151–169, doi:10.3354/cr025151.

Saji, N. H., B. N. Goswami, P. N. Vinayachandran, and T. Yamagata (1999), A dipole mode in the tropical Indian Ocean, *Nature*, *401*, 360–363.

Schott, F. A., S.-P. Xie, and J. P. McCreary Jr. (2009), Indian Ocean circulation and climate variability, *Rev. Geophys.*, *47*, RG1002, doi:10.1029/2007RG000245.

Schramm, C. T. (1985), Implications of radiolarian assemblages for the Late Quaternary paleoceanography of the eastern equatorial Pacific, *Quat. Res.*, *24*, 204–218, doi:10.1016/0033-5894(85)90007-9.

Webster, P. J., A. M. Moore, J. P. Loschnigg, and R. R. Loben (1999), Coupled ocean-atmosphere dynamics in the Indian Ocean during 1997–98, *Nature*, *401*, 356–360, doi:10.1038/43848.

Wyrtki, K. (1973), An equatorial jet in the Indian Ocean, *Science*, *181*, 262–264, doi:10.1126/science.181.4096.262.

S. C. Clemens, Department of Geological Sciences, Brown University, 324 Brook St., P.O. Box 1846, Providence, RI 02912-1846, USA.

S. De, A. K. Gupta, S. Sarkar, and A. Velu, Department of Geology and Geophysics, Indian Institute of Technology, Kharagpur 721 302, India. (anilg@gg.iitkgp.ernet.in)